



# Enhanced performance of wet compression-resorption heat pumps by using NH<sub>3</sub>-CO<sub>2</sub>-H<sub>2</sub>O as working fluid



V. Gudjonsdottir<sup>a,\*</sup>, C.A. Infante Ferreira<sup>a</sup>, Glenn Rexwinkel<sup>b</sup>, Anton A. Kiss<sup>c</sup>

<sup>a</sup> Process and Energy Laboratory, Delft University of Technology, Leeghwaterstraat 39, 2628 CB, Delft, The Netherlands

<sup>b</sup> Frames, Eikenlaan 237, 2404 BP, Alphen aan den Rijn, The Netherlands

<sup>c</sup> AkzoNobel – Supply Chain, Research & Development, Process Technology ECG, Zutphenseweg 10, 7418 AJ, Deventer, The Netherlands

## ARTICLE INFO

### Article history:

Received 2 September 2016

Received in revised form

25 January 2017

Accepted 10 February 2017

Available online 10 February 2017

### Keywords:

Thermodynamic model

NH<sub>3</sub>-CO<sub>2</sub>-H<sub>2</sub>O mixture

Compression resorption

Heat pumps

Heat recovery

## ABSTRACT

Upgrading waste heat by compression resorption heat pumps (CRHP) has the potential to make a strong impact in industry. The efficiency of CRHP can be further improved by using alternative working fluids. In this work, the addition of carbon dioxide to aqueous ammonia solutions for application in CRHP is investigated. The previously published thermodynamic models for the ternary mixture are evaluated by comparing their results with experimental thermodynamic data, and checking their advantages and disadvantages. Then the models are used to investigate the impact of adding CO<sub>2</sub> to NH<sub>3</sub>-H<sub>2</sub>O in wet compression resorption heat pump applications. For an application where a waste stream is heated from 60 to 105 °C, a COP increase of up to 5% can be attained by adding CO<sub>2</sub> to the ammonia-water mixture, without any risk of salt formation. Additional advantages of adding CO<sub>2</sub> to the ammonia-water mixture in that case are decreased pressure ratio, as well as an increase in the lower pressure level. When practical pressure restrictions are considered the benefits of the added CO<sub>2</sub> become even larger or around 25% increase in the COP. Nonetheless, when the waste stream was considered to be additionally cooled down, no significant benefits were observed.

© 2017 The Authors. Published by Elsevier Ltd. This is an open access article under the CC BY license (<http://creativecommons.org/licenses/by/4.0/>).

## 1. Introduction

One of the measures of the European Council to reduce greenhouse gas emissions is to improve energy efficiency [10]. In Europe industry is responsible for approximately a quarter of the total energy consumption [11]. Integration of heat pumps in the process industry has the potential to drastically reduce energy requirements for many applications [22]. Studies have for example shown that significant energy savings can be achieved with integration of heat pumps with distillation columns [21,28,38,47]. However, the use of industrial heat pumps is still quite limited. According to the International Energy Agency (IEA) one of the main reasons is long payback periods [13]. By increasing the efficiency of industrial heat pumps the payback period can hopefully be decreased.

The goal of heat pumps is to transfer heat from low to high temperature. The coefficient of performance (COP) is therefore

evaluated by the ratio of heat delivered by the heat pump to the work required to deliver that heat [30]. Traditional heat pumps have four components; compressor, condenser, expansion valve and evaporator, see Fig. 1. A compression resorption heat pump (also known as hybrid HP) has a resorber and a desorber instead of the condenser and evaporator. It takes advantage of thermo-chemical sorption processes, and it can achieve high temperature levels and lifts, with a relatively high coefficient of performance (COP). The benefits of CHRP are related to the use of environmentally-friendly refrigerants that can contribute to the improvement of the performance. Specifically for industrial heating processes with large temperature glides CHRP allows energy performance gains of more than 20% as compared to vapor compression heat pumps (VCHP) [46]. The use of a mixture allows lower pressure levels, and condensation and evaporation at gliding temperatures – which can result in higher efficiency. Wet compression has the effect of suppressing vapor superheating, and it can also improve the heat pump efficiency. Ammonia-water mixtures can be used as efficient working fluids in CHRP, showing a number of advantages: higher COP because of the use of non-isothermal phase transition of the mixture in the heat exchangers at constant pressure; the mixture allows the achievement of high temperature operation at relatively

\* Corresponding author.

E-mail addresses: [V.Gudjonsdottir@tudelft.nl](mailto:V.Gudjonsdottir@tudelft.nl) (V. Gudjonsdottir), [g.rexwinkel@frames-group.com](mailto:g.rexwinkel@frames-group.com) (G. Rexwinkel), [Tony.Kiss@akzonobel.com](mailto:Tony.Kiss@akzonobel.com) (A.A. Kiss).

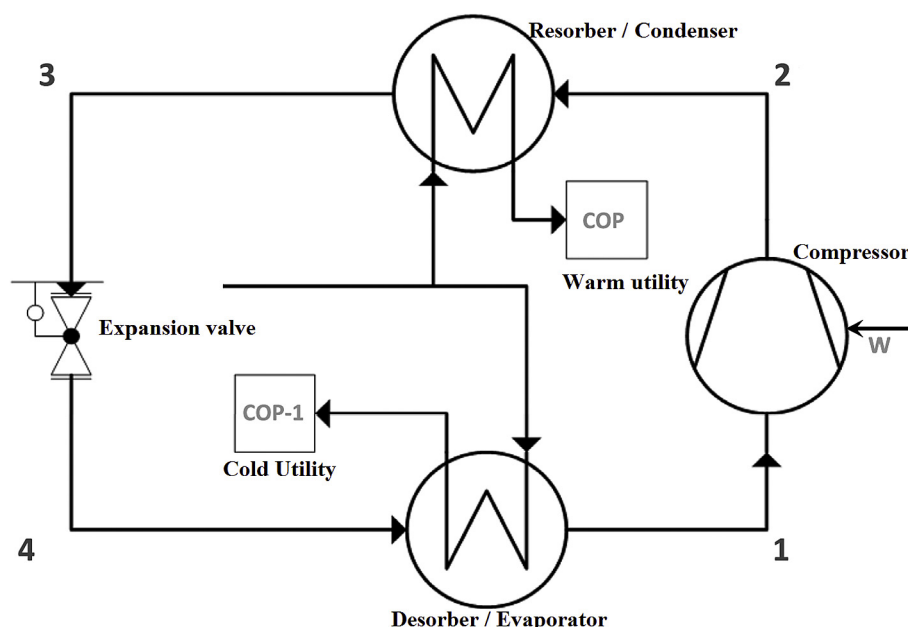


Fig. 1. A schematic of a heat pump; splitting a cooling water return stream into a warm and cold utility stream using a Compression-Resorption Heat Pump.

low operating pressures; the cycle can be designed to show a temperature glide in the resorber that corresponds to the temperature glide of the industrial flow that has to be heated.

Recently, van de Bor and Infante Ferreira [44] proposed a simplified method for the selection of industrial heat pumps taking the major thermodynamic losses into account, and concluded that in the presence of large temperature glides of process stream that needs to be heated, compression resorption heat pumps (CRHP) lead to significant advantages compared to other heat pump technologies. van de Bor et al. [46] have investigated the potential of several alternative technologies to recover low temperature waste heat. The study focused on temperature levels of 45–60 °C since large amounts of (waste) heat are rejected to the environment at these conditions. Wet compression resorption heat pump using ammonia-water as the working fluid shows the best performance in comparison to other alternatives when water is heated up from 60 °C to 105 °C [46]. Recently Jensen et al. [17,18] have extensively studied the technical and economic domains of CRHPs based on the Osenbrück cycle. The wet CRHPs considered in this paper are different since the whole process takes place in the two phase region.

The absorption of carbon dioxide in aqueous ammonia has been proposed in the past years as an improved carbon capture technology. Preliminary studies by Asbroek and Rexwinkel [40] have indicated that this ternary mixture may also lead to positive effects when applied to compression resorption cycles. In the past several working fluids (fluids that circulate through the thermodynamic cycle and transmit energy) have been investigated for application in CRHP [15,48] however this ternary mixture has not been previously proposed. This is actually the motive for the present investigation.

To further investigate the performance of the CRHP with  $\text{NH}_3\text{-CO}_2\text{-H}_2\text{O}$  mixture as a working fluid an accurate thermodynamic model is needed, as the solid base of any process simulation is represented by the physical properties models. Missing or inadequate physical properties can undermine the accuracy of a model or even prevent one from performing the simulation [4]. Different thermodynamic models have been used and developed for calculating the thermodynamic properties of  $\text{NH}_3\text{-CO}_2\text{-H}_2\text{O}$ . These models are normally activity coefficient models for the liquid phase and an equation of state (EOS) for the vapor phase calculations. The

activity coefficient models that have been most commonly used are electrolyte models such as: the Pitzer model [24], the extended UNIQUAC model originally developed by Thomsen and Rasmussen [41] and the more commonly used e-NRTL model proposed by Chen et al. [5]. Darde et al. [8] compared a built in e-NRTL model from Aspen Plus to an upgraded version of the extended UNIQUAC model described by Darde et al. [9]. Their findings were that the extended UNIQUAC model generally performed better than the e-NRTL model from Aspen Plus, especially for the partial pressure of  $\text{NH}_3$  and the solubility of ammonium bicarbonate. Darde [7] mentions that if the binary interaction parameters were better fitted to experimental data for  $\text{NH}_3\text{-CO}_2\text{-H}_2\text{O}$  mixture, the e-NRTL model might become more competitive compared to the extended UNIQUAC model. Since then, the e-NRTL model has been modified in this way by a couple of authors, including Refs. [32,36]. Both of their adjusted models have been used by other authors, for process modeling. For example Zhang and Guo [50] used the model with adjusted parameters from Refs. [27,32] used the modified model from Que and Chen [36].

The extended UNIQUAC model has previously not been compared to the modified model from Que and Chen [36] over a large range of operating conditions. Therefore, in this paper these models are compared together to see if a modified e-NRTL model can perform with similar accuracy as the extended UNIQUAC model. The e-NRTL models that are built into Aspen Plus are used as a reference. Additionally a new fit of the e-NRTL model was developed with an extended application range to be able to more accurately evaluate the impact of added  $\text{CO}_2$  to ammonia water in CRHPs. These thermodynamic models are used to predict the COP of wet CRHP systems which operate under conditions similar to the conditions investigated by van de Bor et al. [46]. The set of equations proposed in that paper to predict the cycle performance has been used to determine the different state conditions when the ternary mixture is used instead of ammonia-water. The results are compared with the performance of the ammonia-water system so that the advantages of the ternary mixture become evident.

Summarizing, this study investigates the effect of adding  $\text{CO}_2$  to the working fluid of wet compression resorption heat pumps which work with ammonia-water. For this purpose, first the

thermodynamic properties of the ternary mixture  $\text{NH}_3\text{-CO}_2\text{-H}_2\text{O}$  are investigated by comparing the extended UNIQUAC model with modified and improved e-NRTL models over a large range of operating conditions. These models, especially e-NRTL models, have been the most commonly used models for the thermodynamic properties of the  $\text{NH}_3\text{-CO}_2\text{-H}_2\text{O}$  mixture in literature. Additionally a new fit is made to further improve the e-NRTL model (extend its application range). Then these properties are used to predict the performance of the mixture when applied in wet CRHP making use of a model that takes into account the major irreversibility's of the cycle: driving forces for heat transfer and deviation from isentropic compression. A case relevant for the process industry is investigated: bringing waste stream to temperature above 100 °C. The results indicate promising enhancement for the COP, pressure ratio, and the pressure levels for certain applications. This solution has therefore the potential to make a strong impact in the industry; increasing the energy efficiency of many processes and in that way reducing emissions.

## 2. Thermodynamic property models

In the next subsections the extended UNIQUAC and the e-NRTL models are described in more detail, covering their applicability ranges as well as their benefits and drawbacks.

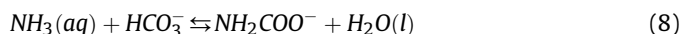
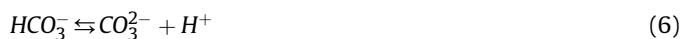
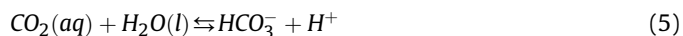
### 2.1. Extended UNIQUAC model

The extended UNIQUAC model was developed by Thomsen and Rasmussen [41]. The model uses the extended UNIQUAC model to calculate activity coefficients for the liquid phase and the Soave-Redlich-Kwong (SRK) EOS for vapor phase calculations. The model was further developed and described by Darde et al. [9] and implemented as a FORTRAN subroutine in Aspen Plus by Maribo-Mogensen [29]. The original model describes accurately the thermodynamic properties of the  $\text{NH}_3\text{-CO}_2\text{-H}_2\text{O}$  mixture for ammonia concentrations up to 80 molal  $\text{NH}_3$  (80 mol  $\text{NH}_3$  per kg solvent, which is water in this case), temperature of 0–110 °C and pressure up to 10 MPa Darde, [7]. The newer version of the model describes the thermodynamic properties accurately up to 150 °C. Additionally the model parameters have been fitted to more experimental data to increase accuracy. The deviation of the experimental data and the model are in general less than 10% except for pressure data at temperatures around and above 100 °C where they are slightly higher. The extrapolation of equilibrium constants into the supercritical range was also improved using Henry's law instead of the Gibbs-Helmholtz equation. The chemical equilibria that are taken into account in the model are the following.

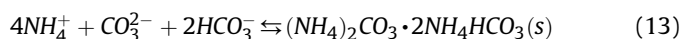
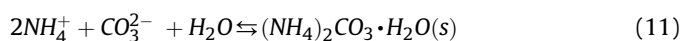
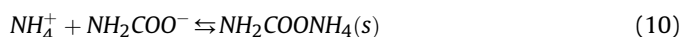
#### 2.1.1. Vapor-liquid equilibrium



#### 2.1.2. Speciation equilibrium



### 2.1.3. Liquid-solid equilibrium



### 2.2. e-NRTL model

The e-NRTL model (electrolyte Non Random Two Liquid) is built into the Aspen Plus software [3]. In this study, version 8.8 of Aspen Plus is used. A data package for  $\text{NH}_3\text{-CO}_2\text{-H}_2\text{O}$  mixture using the e-NRTL method and the Redlich-Kwong (RK) EOS for the vapor phase is included in the software. This model will be called e-NRTL1 from here on. A modified version of the model and the one that Darde et al. [8] used for their comparison are included in a carbon capture example Aspen Physical Property System [1] also included in the Aspen Plus v8.8 software. Additionally this model (called here e-NRTL2) has been regressed to vapor-liquid equilibrium (VLE), solid-liquid equilibrium (SLE), speciation and heat capacity data.

The thermodynamic model proposed by Que and Chen [36] is included in another carbon capture example available in the Aspen Plus software [2]. The main difference between that model and the e-NRTL2 model is that the PC-SAFT (Perturbed Chain Statistical Association Fluid Theory) EOS is used for vapor phase calculations instead of the RK EOS and the model parameters have been fitted to more experimental data. As mentioned in the introduction, the e-NRTL model has also been modified by other authors like Niu et al. [32]. The model modified by Que and Chen [36] was however chosen since more experimental data are used for data regression of the model parameters. The model by Que and Chen [36] is reported to be accurate for systems with temperatures up to 473 K, pressures up to 7 MPa,  $\text{NH}_3$  concentration up to 30 wt%, and  $\text{CO}_2$  loading (molar ratio between  $\text{CO}_2$  and  $\text{NH}_3$ ) up to unity. The average relative deviations between the experimental data and the model results were reported to be lower than 5% for the pressure,  $\text{NH}_3$  and  $\text{CO}_2$  composition.

In the e-NRTL model, only the formation of ammonium bicarbonate ( $\text{NH}_4\text{HCO}_3$ ) is considered for SLE and not ammonium carbonate ( $(\text{NH}_4)_2\text{CO}_3 \cdot \text{H}_2\text{O}$ ), ammonium carbamate ( $\text{NH}_2\text{COONH}_4$ ) and ammonium sesqui-carbonate ( $(\text{NH}_4)_2\text{CO}_3 \cdot 2\text{NH}_4\text{HCO}_3$ ). However, researchers have shown that ammonium bicarbonate is dominant in the total amount of ammonium salts once the  $\text{CO}_2$  absorption reaches steady state [20,33]. Therefore the e-NRTL

model might still be a good option. However since no solid formations are wanted in the CRHP, since they will cause blockage in the system components, further investigation of this point is needed.

These versions of the e-NRTL models are compared to the extended UNIQUAC model as well as a new fit in the following section, where it is demonstrated that the model developed by Que and Chen [36] shows satisfactory results except for SLE at temperatures above 50 °C and for high ammonia concentrations (the reported maximum limit is 30 wt% NH<sub>3</sub>). The new fit is therefore based on the model from Que and Chen [36] except the e-NRTL model binary interaction parameters  $\tau_{1,ij}$  - see equation (14) - associated with the major species of the electrolyte. That is during the fitting procedure the initial values of the interaction parameters where the ones developed by Que and Chen [36] and then they were refitted to additional SLE and VLE ternary NH<sub>3</sub>-CO<sub>2</sub>-H<sub>2</sub>O experimental data. The application range of the new fit is therefore similar to the model from Que and Chen [36] as well as it should give a better indication for higher ammonia concentrations (above 30 wt%). As explained by Que and Chen [36] the e-NRTL model

requires a non-randomness factor  $\alpha_{ij}$  and asymmetric binary interaction energy parameters  $\tau_{ij}$  calculated with the next equation:

$$\tau_{ij} = \tau_{1,ij} + \frac{\tau_{2,ij}}{T} \quad (14)$$

where  $i$  and  $j$  stand for the components, either ionic species, water, ammonia or carbon dioxide. An overview of the experimental data is listed in Table 1 and the refitted parameters are listed in Table 2.

### 3. Comparison of thermodynamic property models

The selected model should be able to describe the VLE, the SLE, speciation and enthalpy change over a large range of temperatures and concentrations of NH<sub>3</sub> and CO<sub>2</sub> to be able to accurately simulate an NH<sub>3</sub>-CO<sub>2</sub>-H<sub>2</sub>O heat pump system. Comparison of the models mentioned previously, are discussed in the following sections.

#### 3.1. Vapor-liquid equilibrium

The partial bubble point pressures of CO<sub>2</sub> and NH<sub>3</sub> versus the molality of CO<sub>2</sub> based on the different models and the new fit are compared for different temperatures in Fig. 2 (20 °C), Fig. 3 (40 °C), Fig. 4 (120 °C) and Fig. 5 (150 and 160 °C). Additionally the VLE experimental data from Shen [39] and Yanagisawa et al. [49] are compared to the model results from Que and Chen [36]; the extended UNIQUAC model and the new fit in Fig. 6.

The e-NRTL1 model is generally inaccurate at high temperatures and high loadings, as previously reported by Darde [7]. The e-NRTL2 model is in most cases an improvement from the e-NRTL1 model, but it generally underestimates the partial bubble point pressure of NH<sub>3</sub>, as well as inaccurately portrays the CO<sub>2</sub> pressure at high loadings at 20 and 40 °C. The model by Que and Chen [36]; the new fit and the extended UNIQUAC model quite accurately portray the partial pressures at low molalities of NH<sub>3</sub>. Jilvero et al. [19] even reported that the model by Que and Chen [36] fits their experimental data of CO<sub>2</sub> partial bubble point pressures, for 10–40 °C, even more accurately than the extended UNIQUAC model. At higher molalities of NH<sub>3</sub> the models start to underestimate the pressure as can be seen most clearly from Figs. 4 and 6. As mentioned before the limit of the model by Que and Chen [36] is reported to be 30 wt % NH<sub>3</sub> (approximately 24 molal NH<sub>3</sub>). The limit of the original extended UNIQUAC model was reported by Darde [7] as 80 molal NH<sub>3</sub>. The newer version of the model that Darde [7] uses is however refitted with data that does not come close to that limit. And it is quite clear, especially from Fig. 6, that the newer model under

**Table 1**  
Experimental data for regression of the NH<sub>3</sub>-CO<sub>2</sub>-H<sub>2</sub>O system.

Data Type	$T, K$	wt% $\text{NH}_4\text{HCO}_3$		Source	
SLE	273–363	2.4–14.4		[16]	

Data Type	$T, K$	mol% $\text{NH}_3$	mol% $\text{CO}_2$	$P \text{ (MPa)}$	Deviation (%)	Source
VLE	393.15	1.2–17.7	0.3–9.9	0.3–5	6.6	[12]
VLE	393.15	4–18	0.4–7.6	0.1–1.3	7.1	[31]
VLE	343–371	47.5–62.8	6.5–13.5	1.96	7.7	[49]
VLE	303–333	10.8–66.3	1.8–6.1	0.02–2.1	12.7	[39]

**Table 2**  
Adjusted NRTL binary interaction parameters.

Component <i>i</i>	Component <i>j</i>	$\tau_{1,ij}$
H <sub>2</sub> O	(NH <sub>4</sub> <sup>+</sup> , HCO <sub>3</sub> <sup>-</sup> )	-4.27128
H <sub>2</sub> O	(NH <sub>4</sub> <sup>+</sup> , CO <sub>3</sub> <sup>2-</sup> )	3.29344
(NH <sub>4</sub> <sup>+</sup> , CO <sub>3</sub> <sup>2-</sup> )	H <sub>2</sub> O	-2.82125
H <sub>2</sub> O	(NH <sub>4</sub> <sup>+</sup> , NH <sub>2</sub> COO <sup>-</sup> )	9.73284
(NH <sub>4</sub> <sup>+</sup> , NH <sub>2</sub> COO <sup>-</sup> )	H <sub>2</sub> O	-4.39773
NH <sub>3</sub>	(NH <sub>4</sub> <sup>+</sup> , NH <sub>2</sub> COO <sup>-</sup> )	7.82722
(NH <sub>4</sub> <sup>+</sup> , NH <sub>2</sub> COO <sup>-</sup> )	NH <sub>3</sub>	-4.58504

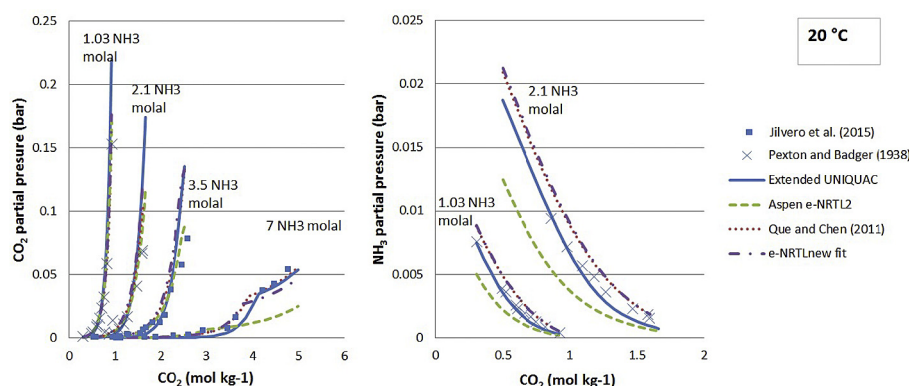


**Fig. 2.** Comparison of the experimental data for partial bubble point pressures of CO<sub>2</sub> and NH<sub>3</sub> at 20 °C with the model correlations [35].



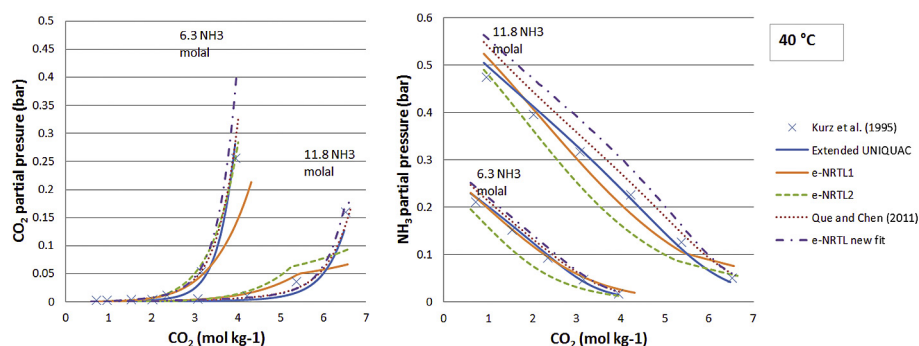


Fig. 3. Comparison of the experimental data for partial bubble point pressure of  $\text{CO}_2$  and  $\text{NH}_3$  at 40 °C with the model correlations.

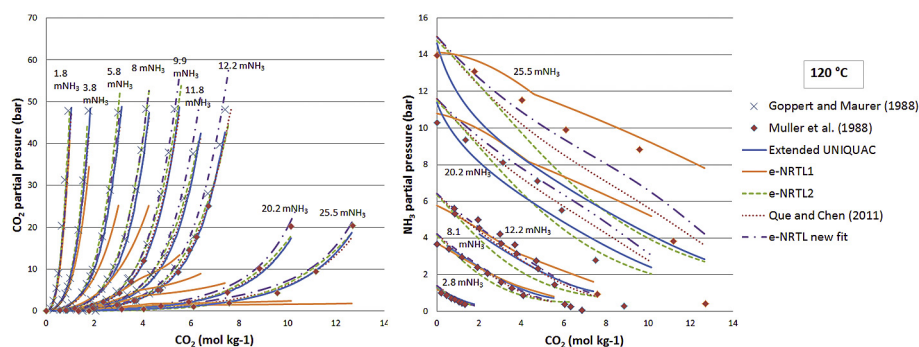


Fig. 4. Comparison of the experimental data for partial bubble point pressure of  $\text{CO}_2$  and  $\text{NH}_3$  at 120 °C with the model correlations.

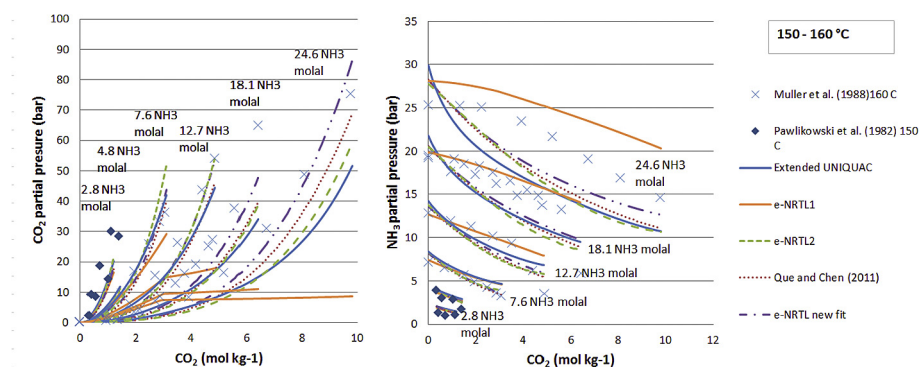


Fig. 5. Comparison of the experimental data for partial bubble point pressure of  $\text{CO}_2$  and  $\text{NH}_3$  at 150 and 160 °C with the model correlations [34].

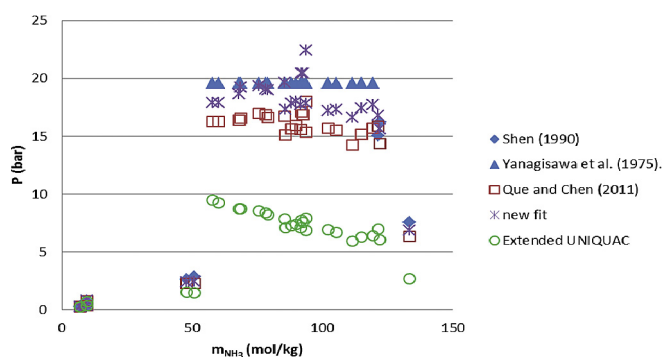


Fig. 6. Comparison of the experimental data from Shen [39] and Yanagisawa et al. [49] for bubble point pressure with the model correlations.

predicts the pressure at concentrations above approximately 30 wt %  $\text{NH}_3$ . The new fit corresponds most accurately to the experimental data at these higher concentrations.

### 3.2. Solid-liquid equilibrium

The comparison of the models for solubility of ammonium bicarbonate ( $\text{NH}_4\text{HCO}_3$ ) in water versus temperature is shown in Fig. 7. The models are compared to experimental data from Refs. [16,43] and Toporescu [42]. Assuming that the experimental data from Janecke [16] is accurate, the extended UNIQUAC models, as well as the new fit are the most accurate at high temperatures or above approximately 50 °C. At higher temperatures, the e-NRTL2 and the model proposed by Que and Chen [36] overestimate the solubility of  $\text{NH}_4\text{HCO}_3$ . The e-NRTL1 model, similar to the trend seen from the VLE data, deviates from the experimental data at high temperatures and high loadings, in this case around 70 °C. In the

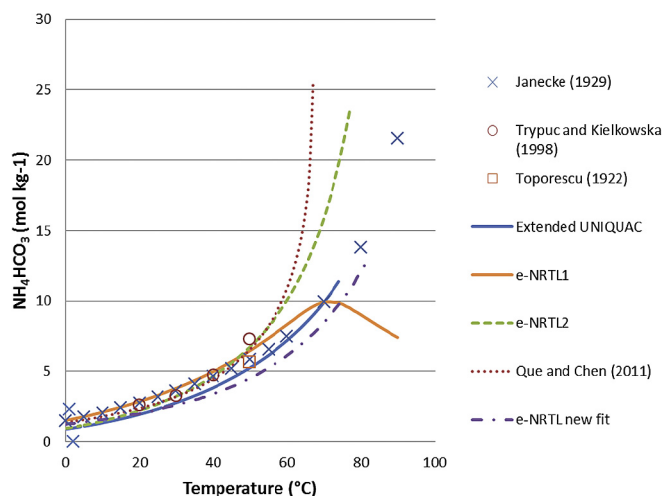


Fig. 7. Comparison of the experimental data for solubility of  $\text{NH}_4\text{HCO}_3$  in water with the model predictions.

case of e-NRTL2 and the model from Que and Chen [36] the reason for this difference can be easily explained since the experimental data used for the regression for both models was the one from Trypuc and Kielkowska [43]. The experimental data from them reaches to temperatures of 50 °C. Also their value at 50 °C is slightly higher than the one from Janecke [16] and Toporescu [42]. Since more experimental data at high temperatures was not found in literature it is questionable which of the data sets corresponds best to reality. Additionally in practice for the CRHP application the concentration of  $\text{NH}_3$  and  $\text{CO}_2$  is unlikely to come close to the concentration necessary for ammonium bicarbonate formation at

high temperatures. For example the reported concentration by Janecke [16] of  $\text{CO}_2$  at approximately 60 °C is around and above 30 wt% (depending on the  $\text{NH}_3$  concentration). The data from Trypuc and Kielkowska [43] suggest that this limit might be even higher and therefore either model should give satisfying results if the application concentration does not reach this limit.

### 3.3. Speciation

Comparison of speciation calculations of the models and experimental data from Lichtfers [26] is shown in Figs. 8 and 9. All the models are able to quite accurately describe the speciation at both temperatures (60 and 120 °C, respectively) except the e-NRTL2 model. The e-NRTL2 model overestimates the concentration of ammonia and bicarbonate and underestimates the carbamate concentrations. In the two previous subsections, the e-NRTL2 model was in general an improvement of the original model (e-NRTL1). This shows the importance of using a wide range of experimental data for parameter fitting for the  $\text{NH}_3\text{-CO}_2\text{-H}_2\text{O}$  system.

### 3.4. Enthalpy change

In Figs. 10–12 the models are compared to experimental data from Rumpf et al. [37] for enthalpy change upon partial evaporation of the  $\text{NH}_3\text{-CO}_2\text{-H}_2\text{O}$  mixture. The temperature range of the experiments was from 40 to 137 °C with a typical temperature increase of 5–15 °C. The concentration range for  $\text{NH}_3$  was up to 12 molal and up to 6 molal for  $\text{CO}_2$ . The reported temperatures and pressures from Rumpf et al. [37] are used to calculate the inlet enthalpy. At the outlet however the reported vapor fraction is used instead of the pressure since the accuracy of the weight of the liquid and vapor part is higher than that of the measured pressure. All

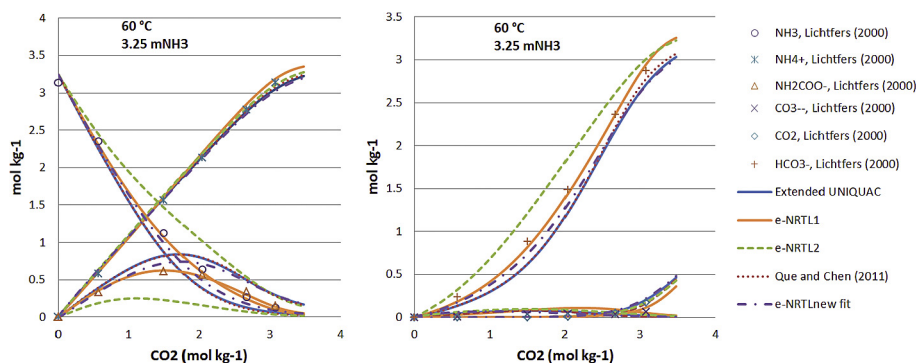


Fig. 8. Comparison of the experimental data for speciation at 60 °C and molality of 3.25 mol/kg  $\text{NH}_3$  with the model correlations.

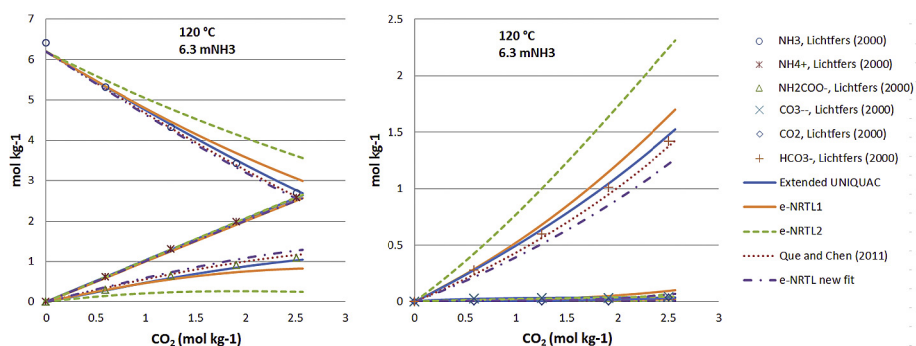


Fig. 9. Comparison of the experimental data for speciation at 120 °C and molality of 6.3 mol/kg  $\text{NH}_3$  with the model correlations.

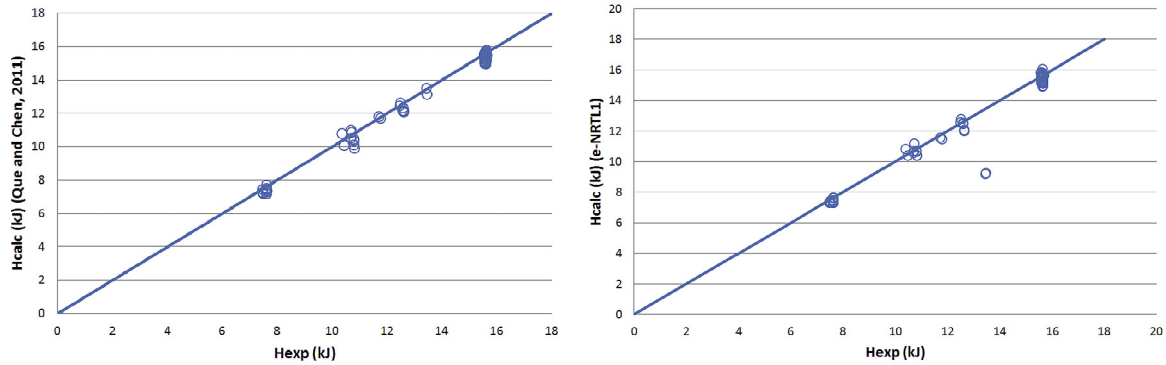


Fig. 10. Comparison of the experimental data from Rumpf et al. [37] for heat of partial evaporation: (left) Que and Chen [36] and (right) e-NRTL1 correlations.

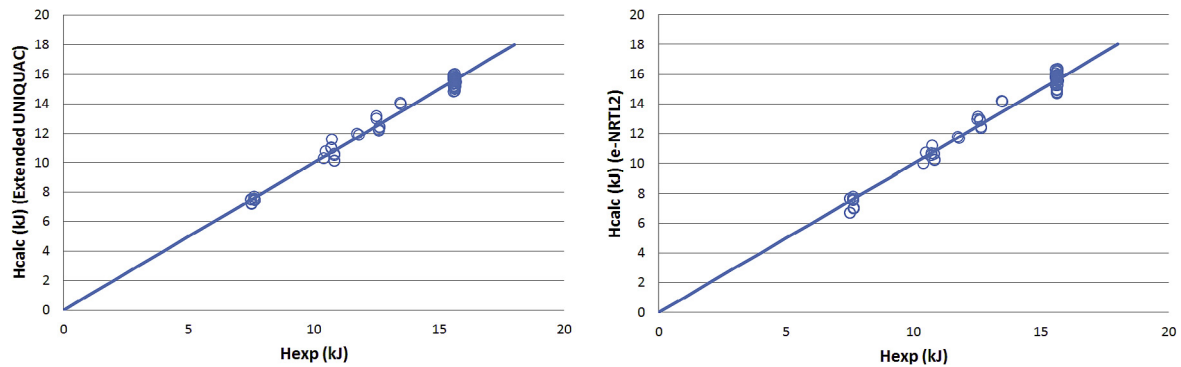


Fig. 11. Comparison of the experimental data from Rumpf et al. [37] for heat of partial evaporation: (left) extended UNIQUAC and (right) e-NRTL2 correlations.

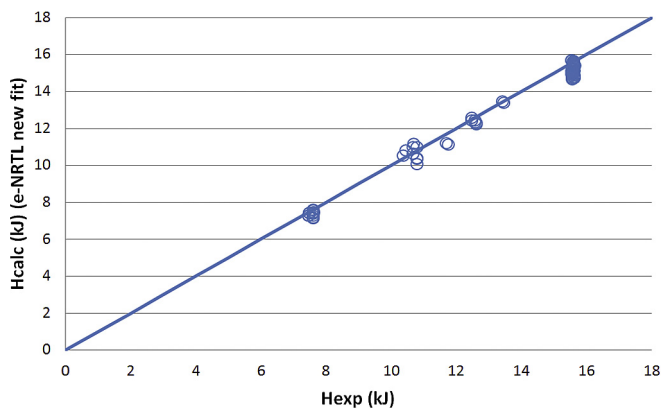


Fig. 12. Comparison of the experimental data from Rumpf et al. [37] for heat of partial evaporation and the e-NRTL new fit correlation.

correlations show good matches to the experimental data, on average the deviation is less than 3%, with the only exception of two points for the e-NRTL1 correlation. These two points were at the highest reported temperature and  $\text{CO}_2$  loading. This deviation corresponds to the previous shown results of VLE and SLE data.

#### 4. Application of $\text{NH}_3\text{-CO}_2\text{-H}_2\text{O}$ mixture to wet compression resorption heat pump

##### 4.1. Model of compression-resorption heat pump

The process for the compression-resorption heat pump is

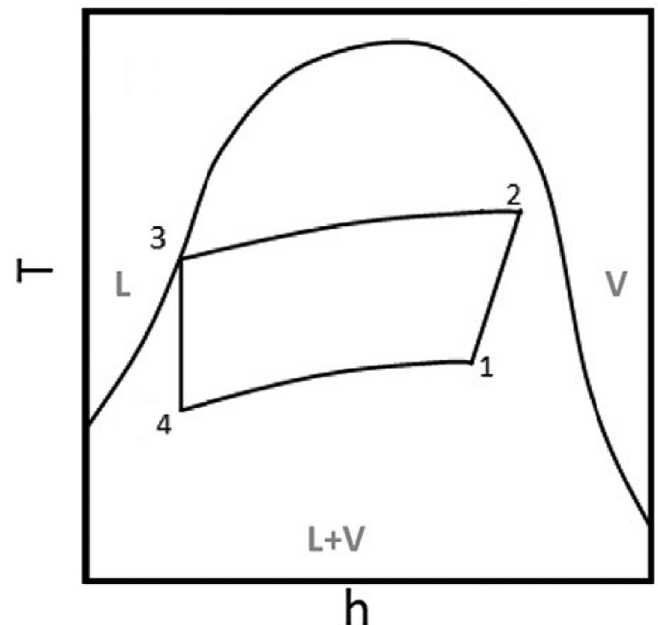


Fig. 13. Typical temperature-enthalpy diagram for compression-resorption heat pumps. Position 1 indicates the process conditions after the desorber, 2 indicate the conditions at the outlet of the compressor, 3 indicates the conditions at the outlet of the resorber and 4 indicates the conditions after the expansion valve [46].

presented in the temperature-enthalpy diagram illustrated in Fig. 13 van de Bor et al. [46]. Fig. 13 gives a representation of the cycle, where  $T_3$  is fixed at the waste stream inlet temperature (for

**Table 3**

Equations used to model the CRHP.

$T_1 = [T_{cw} - \Delta T_{driving}]$
$T_3 = [T_{cw} + \Delta T_{driving}]$
$P_2, P_3, h_3, h_4 = f(T_3, q = 0)$
$T_2, h_2 = f(P_3, q = 1)$
$h_1, s_1 = f(P_1, T_1)$
$h_{2s} = f(P_3, s_1)$
$h_2 = \frac{h_{2s} - h_1}{\eta_c} + h_1$
$COP = (h_2 - h_3)/(h_2 - h_1)$

instance 60 °C) plus 5 K driving force, while  $T_1$  is fixed at the waste stream inlet temperature minus 5 K driving force. The desorber and resorber are additionally divided into 100 control volumes to ensure that the pinch temperature does not become smaller than 5 K. The isentropic efficiency of the compressor is assumed 70%. Infante Ferreira et al. [14] have reported experimental data for wet compression of ammonia-water and have obtained isentropic efficiency up to 35% with a prototype screw compressor. It is expected that further improvement of such compressor will allow for efficiencies of 70% and higher. The optimal vapor quality at the outlet of the compressor for wet compression was investigated by van de Bor et al. [45] for 50 different industrial cases. The optimal solution is to have saturated vapor at the compressor outlet. Therefore for the wet compression cycle,  $P_1$  is initially guessed, from which  $h_1$ ,  $s_1$ ,  $h_{2s}$ , and  $h_2$  are calculated, while  $P_1$  is iterated until  $h_2$  matches the value for saturated vapor at  $P_2$ . For convenience, a summary of equations used to determine the COP of compression resorption heat pumps is given in Table 3. Note that, for what concerns ammonia-water, the model was developed using NIST RefProp version 9.1 [25]. For the  $\text{NH}_3\text{-CO}_2\text{-H}_2\text{O}$  calculations the extended UNIQUAC [9], the modified model by Que and Chen [36] and the new fit based on their model are used.

#### 4.2. Operating conditions of the reference heat pump

The case considered concerns the heating of a water waste stream flow from 60 °C to 105 °C while part of the stream is cooled down in the desorber. The flow is assumed to be sufficient to achieve the desired temperature levels. Fig. 1 illustrates the situation. In the first example the focus is only on heating (with a temperature lift of 55 K), while in the second example this case is expanded to consider additionally that the waste stream is partly cooled down from 60 °C to 15 °C.

#### 4.3. Comparison of cycle performance

##### 4.3.1. Heating case

The benefits of adding  $\text{CO}_2$  to the ammonia-water mixture of the case where a waste stream is heated from 60 °C to 105 °C are illustrated in Figs. 14 and 15 and an example of the cycle calculations results are listed in Tables 4 and 5. The observed trend in the cycle performance with an ammonia water mixture is that an optimum exists when the working fluid temperature glide is fitted to the heat sink rather than the heat source. This same trend was observed by van de Bor et al. [45] where 50 industrial cases were investigated. This optimum is in this case for an ammonia weight fraction of 19.1%. When  $\text{CO}_2$  is added the ammonia concentration has to be increased to achieve the optimum cycle performance. For example, at 20 wt%  $\text{CO}_2$  the  $\text{NH}_3$  concentration is 31.2% according to the calculations with the extended UNIQUAC model and 24.6% with the model from Que and Chen [36]; see Table 4.

Fig. 14 plots the COP versus the  $\text{CO}_2$  weight fraction. The models show the same trend: the COP increases with increased  $\text{CO}_2$

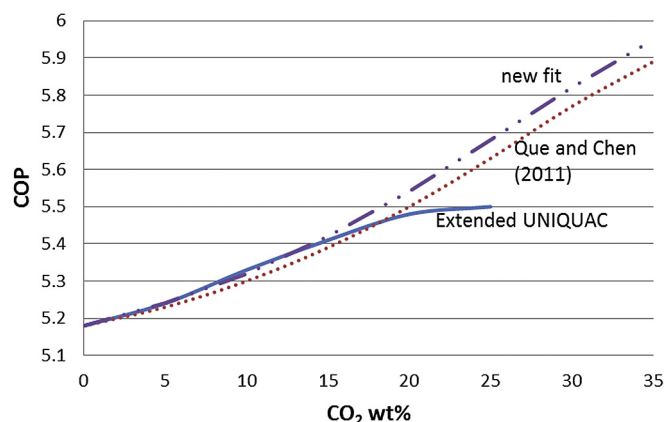


**Fig. 14.** COP vs  $\text{CO}_2$  weight fraction, heating case. Results from the extended UNIQUAC model are shown with continuous line; the model of Que and Chen [36] with dotted line, and the new fit with dashed line.

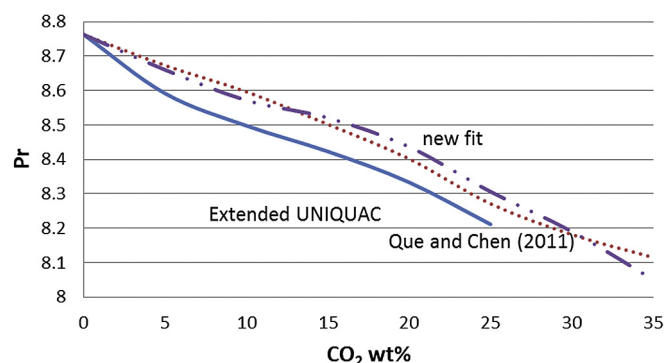


**Fig. 15.** Pressure ratio vs  $\text{CO}_2$  weight fraction, heating case. Results from the extended UNIQUAC model are shown with continuous line; the model of Que and Chen [36] with dotted line, and the new fit with dashed line.

concentration. However, the extended UNIQUAC model predicts salt formation (ammonium carbonate) around 18 wt%  $\text{CO}_2$  in the stream after the valve (at the lowest temperature in the cycle). At this point the increase in COP reduces. In practice, any salt formation is unwanted in the cycle since it will eventually cause a blockage. The modified e-NRTL models predict no salt formation until above 35 wt%  $\text{CO}_2$ . As mentioned earlier the e-NRTL models only predict if there is a formation of ammonium bicarbonate. If there is indeed ammonium carbonate forming this shows a clear advantage of the extended UNIQUAC model over the e-NRTL models. The increase in COP with added  $\text{CO}_2$  before any salt formation is predicted is around 5%. A traditional VCHP operating with ammonia would have a COP around 4 in this case. The improvement of a CRHP operating with ammonia and water is already around 30% and with the addition of  $\text{CO}_2$  the improvement comes close to 40%. Assuming a compressor efficiency of 70% will be attainable.

The pressure ratio is plotted versus the  $\text{CO}_2$  weight fraction in Fig. 15 and the absolute pressure results are listed in Table 4. From the figure and the table it is clear that the benefits of adding  $\text{CO}_2$  is not only the increase in COP, but also the pressure ratio decreases and the lower pressure level increases. For the ammonia-water case the lower pressure level is about 0.2 bar for the optimum case, which can be difficult to achieve in practice. The pressure can be increased at higher ammonia concentration, but then the COP decreases. The benefits of the added  $\text{CO}_2$  can be even greater if there are any pressure restrictions of the lower pressure level.



**Table 4**

Mixture composition, temperature and pressure results for the CRHP cycle for the heating case.

Model	wt%			T <sub>1</sub> (°C)	T <sub>2</sub> (°C)	T <sub>3</sub> (°C)	T <sub>4</sub> (°C)	P <sub>low</sub> (bar)	P <sub>high</sub> (bar)
	NH <sub>3</sub>	H <sub>2</sub> O	CO <sub>2</sub>						
Refprop	19.1	80.9	0	55	110	65	24.8	0.202	1.77
Refprop	39.3	60.7	0	55	143.2	65	3.5	0.3	6.42
Extended UNIQUAC	31.2	48.8	20	55	110	65	20.8	0.3	2.5
[36]	24.6	55.4	20	55	110	65	26.7	0.269	2.26
[36]	29.2	50.8	20	55	119.7	65	17.5	0.3	3.345
New fit	22.8	57.2	20	55	110	65	28.9	0.259	2.185
New fit	28.7	51.3	20	55	123.9	65	16	0.3	3.79

**Table 5**

Mixture composition, enthalpy and COP results for the CRHP cycle for the heating case.

Model	wt%			h <sub>1</sub> (kJ/kg)	h <sub>2</sub> (kJ/kg)	h <sub>3</sub> (kJ/kg)	h <sub>4</sub> (kJ/kg)	COP
	NH <sub>3</sub>	H <sub>2</sub> O	CO <sub>2</sub>					
Refprop	19.1	80.9	0	2081.9	2533.2	194.7	194.7	5.18
Refprop	39.3	60.7	0	1780.7	2413.8	187.6	187.6	3.52
Extended UNIQUAC	31.2	48.8	20	−9442.9	−9047.9	−11211.3	−11211.3	5.48
[36]	24.6	55.4	20	−10156.6	−9763.3	−11926.7	−11926.7	5.5
[36]	29.2	50.8	20	−9704.4	−9259.4	−11396.9	−11396.9	4.8
New fit	22.8	57.2	20	−10348.5	−9955.1	−12135.0	−12135.0	5.54
New fit	28.7	51.3	20	−9773.1	−9307.3	−11452.6	−11452.6	4.61

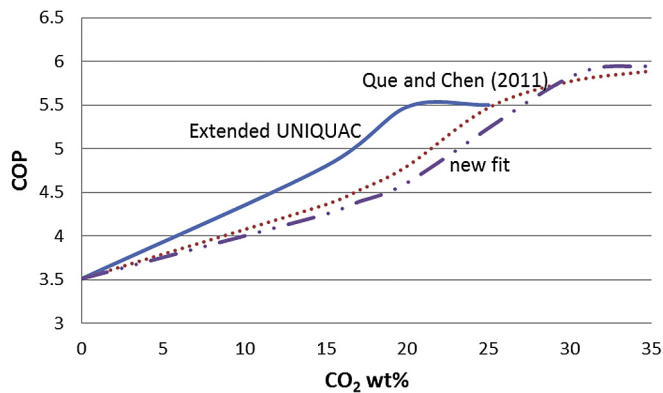
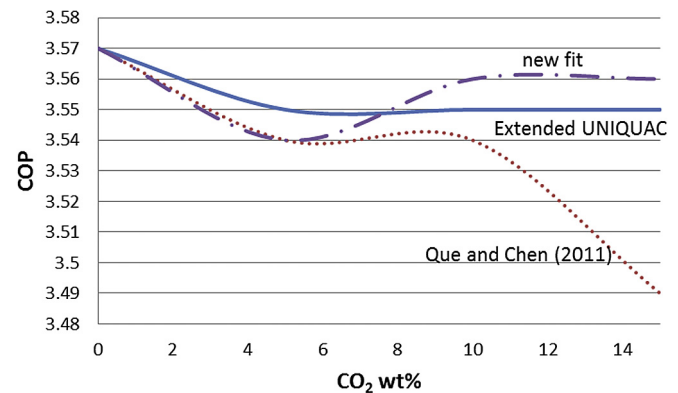
**Fig. 16.** COP vs CO<sub>2</sub> weight fraction, 0.3–25 bar pressure limit. Results from the extended UNIQUAC model are shown with continuous line; the model of Que and Chen [36] with dotted line, and the new fit with dashed line.

Fig. 16 plots the COP versus the CO<sub>2</sub> weight fraction when the pressure level is restricted from 0.3 bar (shaft seal requirements limitation) to 25 bar (equipment cost limitation), a pressure range which is more easily reached in practice. The higher pressure restriction is included since another local optimum exists when the temperature glide is fitted to the heat source rather than the heat sink. This local optimum is found at higher ammonia weight fraction where the pressure levels become way higher which would require specialized and more expensive equipment. From Fig. 17 it is clear that the benefits of the added CO<sub>2</sub> are now much larger. It should be noted that the ammonia weight fraction is around and above 30 wt%, see Table 4, and therefore the modified model by Que and Chen [36] and the extended UNIQUAC model are reaching their limits. The new fit estimates an improvement of 25% in the COP compared to the ammonia water system before the extended UNIQUAC model predicts solid formations (around 18 wt% CO<sub>2</sub>).

When CO<sub>2</sub> is added to the ammonia-water mixture the heat exchanger area decreases for the same heat output for the

**Fig. 17.** COP vs CO<sub>2</sub> weight fraction, cooling included. Results from the extended UNIQUAC model are shown with continuous line; the model of Que and Chen [36] with dotted line, and the new fit with dashed line.

optimized case. The pressure ratio and electricity cost are also lower therefore the payback period should be shorter than for a CRHP operating with ammonia-water.

In the case where the lower pressure is restricted the area increases slightly with added CO<sub>2</sub>. The reason is that the temperature difference in the resorber is smaller with the added CO<sub>2</sub> which means that the needed heat transfer area is larger. However the decrease in pressure ratio and the increase in COP are even higher in this case. Therefore the payback period should still be shorter in this case compared to an CRHP operating with ammonia-water.

The corrosion risk might however increase with the added CO<sub>2</sub>. In water - CO<sub>2</sub> system the largest cause for corrosion is carbonic acid, H<sub>2</sub>CO<sub>3</sub> [6]. With enough ammonia included, as is the case here, this acid should however not be formed. Also according to Krzemień et al. [23] the main causes for corrosion in amine-based CO<sub>2</sub> capture processes are oxidizing acid species like NO<sub>x</sub> and SO<sub>x</sub> and heavy metals in the amine solution. Therefore the risk of corrosion for this mixture might be comparable to that of

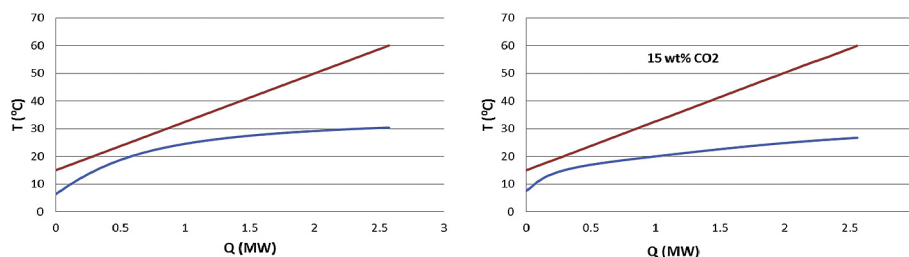


Fig. 18. Temperature profiles in the desorber. Left: profiles for the ammonia water mixture. Right: added CO<sub>2</sub> (15 wt%) calculated with the new fit.

ammonia-water. Further investigation is however needed to confirm this.

#### 4.3.2. Additional cooling case

The same case is now considered except that now an extra cooling demand is assumed. That is the waste water stream is assumed to be partly cooled down to 15 °C. Since the same heat sink is assumed the optimum ammonia weight fraction is still 19.1%, for an ammonia water mixture, and the acquired COP is 3.58. However to reach the required cooling demand the lower pressure level is significantly lower or around 0.057 bar. This pressure level is quite difficult to reach in practice. If the lower pressure level is restricted to 0.3 bar the necessary ammonia weight fraction increases to 40 wt% NH<sub>3</sub> and the COP decreases to 2.97. However in that case the temperature glide of the ammonia water mixture is of course not fitted optimally to the heat sink. In this case the optimal weight fraction will actually become 91.1 wt% NH<sub>3</sub> which results in a COP of 3.29, in this case the temperature glide of the ammonia water

mixture is fitted to the heat source rather than the heat sink. Adding CO<sub>2</sub> will not be beneficial with an ammonia weight fraction this high, since there is not enough water. This is therefore not the optimal application case for adding CO<sub>2</sub>, it is however interesting to test the boundaries of the models and to investigate the potential benefits of added CO<sub>2</sub>. Fig. 17 plots the COP versus the CO<sub>2</sub> weight fraction when it is assumed that there are no limits to the lower pressure level. In this case the models all predict a decrease in the COP with added CO<sub>2</sub> and additionally the pressure ratio increases. This is likely due to the fact that the temperature glide of the NH<sub>3</sub>-CO<sub>2</sub>-H<sub>2</sub>O mixture does not fit as well to the temperature glide in the desorber as that of the ammonia water mixture (see Fig. 18).

Fig. 19 plots the COP versus the CO<sub>2</sub> weight fraction when there is a 0.3 bar limit for the lower pressure level and an example of the cycle calculations results are listed in Tables 6 and 7 with and without pressure limits. The models from Que and Chen [36] and the new fit show similar results as before, that is there is hardly any improvement of the cycle performance with added CO<sub>2</sub>. In contrast, the extended UNIQUAC model in this case shows an improvement of the COP. However as was shown in section 3.1 the model does not accurately predict experimental data for these ammonia weight fractions (approximately 50 wt% NH<sub>3</sub>). It is therefore highly unlikely that the model results are accurate. However it can give an indication of the formation of solids. For the present condition, the model predicts ammonium carbonate formation before 10 wt% of CO<sub>2</sub>. This is not surprising since now the lowest temperature level in the cycle is lower than for the case when only heating is considered. It should be noted that also for conventional heat pumps the simultaneous delivery of hot and cold output leads to higher pressure ratios and very low COPs. For instance, a butane heat pump would require a pressure ratio of 12.4 and have a COP of only 1.8. Therefore an CRHP operating with ammonia water mixture can already improve the process significantly.

## 5. Results analysis and discussion

The comparison of the thermodynamic models shows that the

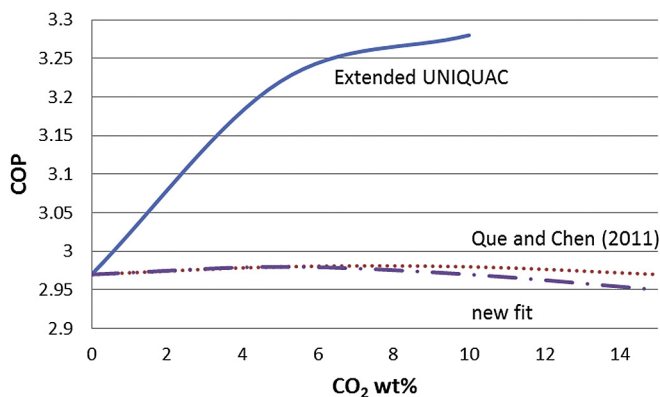


Fig. 19. COP vs CO<sub>2</sub> weight fraction, cooling included and 0.3 bar lower pressure limit. Results from the extended UNIQUAC model are shown with continuous line; the model of Que and Chen [36] with dotted line, and the new fit with dashed line.

Table 6

Mixture composition, temperature and pressure results for the CRHP cycle for the cooling case.

Model	wt%			T <sub>1</sub> (°C)	T <sub>2</sub> (°C)	T <sub>3</sub> (°C)	T <sub>4</sub> (°C)	P <sub>low</sub> (bar)	P <sub>high</sub> (bar)
	NH <sub>3</sub>	H <sub>2</sub> O	CO <sub>2</sub>						
Refprop	19.1	80.9	0	30.4	110	65	6.3	0.057	1.77
Refprop	91.1	0.09	0	55	144.8	77.6	10	5.4	35.2
Refprop	49	51	0	49.2	154.3	65	-9.1	0.3	10.2
Extended UNIQUAC	20.3	74.7	5	28.9	110	65	3.99	0.055	1.831
Extended UNIQUAC	44	51	5	48.1	138.7	65	-5.7	0.3	7.209
[36]	19.2	75.8	5	29.0	110	65	5.68	0.055	1.826
[36]	48.6	46.4	5	47.9	152.6	65	-11.3	0.3	10.307
New fit	18.6	76.4	5	28.9	110	65	6	0.054	1.809
New fit	48.2	46.8	5	48	153.2	65	-11.3	0.3	10.389

**Table 7**

Mixture composition, enthalpy and COP results for the CRHP cycle for the cooling case.

Model	wt%			$h_1$ (kJ/kg)	$h_2$ (kJ/kg)	$h_3$ (kJ/kg)	$h_4$ (kJ/kg)	COP
	NH <sub>3</sub>	H <sub>2</sub> O	CO <sub>2</sub>					
Refprop	19.1	80.9	0	1878.9	2533.2	194.7	194.7	3.57
Refprop	91.1	0.09	0	1533.0	1929.5	623.8	623.8	3.29
Refprop	49	51	0	1629.1	2346.1	216.4	216.4	2.97
Extended UNIQUAC	20.3	74.7	5	−11507.0	−10854.4	−13169.9	−13169.9	3.55
Extended UNIQUAC	44	51	5	−8167.2	−7531.0	−9577.0	−9577.0	3.22
[36]	19.2	75.8	5	−11648.7	−11005.8	−13284.0	−13284.0	3.54
[36]	48.6	46.4	5	−8488.2	−7794.6	−9863.2	−9863.2	2.98
New fit	18.6	76.4	5	−11714.5	−1107.8	−13352.0	−13352.0	3.54
New fit	48.2	46.8	5	−8529.43	−7833.63	−9909.88	−9909.88	2.98

modified e-NRTL models are generally an improvement of the original model. The model modified by Que and Chen [36] and the new fit are especially compatible with the extended UNIQUAC model at low ammonia concentrations. The model developed by Que and Chen [36] is even more accurate for the partial pressure of CO<sub>2</sub> at low temperatures (10–40 °C) as reported by Jilvero et al. [19] and at high ammonia concentrations. Their model also improves the partial pressure of NH<sub>3</sub> and speciation compared to the e-NRTL2 model. The exception is the SLE. The model further underestimates the pressure at high ammonia concentrations. The extended UNIQUAC model under predicts the pressure at high NH<sub>3</sub> concentrations even more seriously. The new fit that was developed in this work, based on the model by Que and Chen [36]; solves these problems, and the new model is able to represent the experimental data, in general, satisfactorily. The new fit should therefore be applicable for the same range and applications as the model developed by Que and Chen [36] as well as to give a better indication for higher ammonia concentrations (above 30 wt%). However, ammonium bicarbonate is, as mentioned before, the only solid formation that is predicted by the e-NRTL models.

The NH<sub>3</sub>–CO<sub>2</sub>–H<sub>2</sub>O mixture shows great potential for certain CRHP applications (e.g. heating only). As was shown with the cooling case, not all applications will benefit significantly from adding CO<sub>2</sub>. Each potential application case should therefore be investigated beforehand. A known fact is that there is a larger chance of solid formations at lower temperature levels and the potential benefits of adding CO<sub>2</sub> will therefore be smaller. It should also be noted that the calculations were pushing the reported limits of the models, around and above 30 wt% NH<sub>3</sub>. Also the available experimental data in this range is limited and the data sets are not consistent. Therefore it is difficult to evaluate the error of the predicted COP with the added CO<sub>2</sub>. Therefore experiments to confirm the potentials of the mixture are planned in the near future. These first experiments will test the CRHP cycle, except for the desorber, with ammonia–water as well as NH<sub>3</sub>–CO<sub>2</sub>–H<sub>2</sub>O as working fluids.

## 6. Conclusions

From the model comparison it is clear that the modified e-NRTL models are in general an improvement of the original model. The model modified by Que and Chen [36] and the new proposed fit are especially compatible with the Extended UNIQUAC model for ammonia concentrations below 30 wt%. The exception is the SLE. All models additionally under predict the pressure at higher ammonia concentrations. The new fit that was developed to include experimental data at higher concentrations fits the data with comparable or higher accuracy than the other models. However since there is a risk of formation of other solids than ammonium bicarbonate, the extended UNIQUAC model is in general

recommended for ammonia concentrations below 30 wt%. The NH<sub>3</sub>–CO<sub>2</sub>–H<sub>2</sub>O mixture shows great potential for certain CRHP cycles with wet compression; both the COP can increase as well as the pressure levels and pressure ratio can become more favourable. The benefits of the NH<sub>3</sub>–CO<sub>2</sub>–H<sub>2</sub>O mixture for CRHP will depend on each application case. For the heating case discussed in this study a COP increase of approximately 5% can be attained compared to a cycle operating with only ammonia water without any risk of solid formation. When there are additionally practical pressure restrictions the benefits can become even higher for this application case or around 25% increase in the COP. When the heat pump must also deliver low temperature heat, the benefit of added CO<sub>2</sub> appear to become insignificant. Experiments will be conducted in the near future to further validate the benefits of the NH<sub>3</sub>–CO<sub>2</sub>–H<sub>2</sub>O mixture for CRHP. The experiments will additionally aim to test a prototype compressor that can perform wet compression since a commercial solution is not available at this point.

## Acknowledgements

This is an ISPT (Institute for Sustainable Process Technology) project. The authors are grateful to K. Thomsen and B. Maribo-Mogensen for giving permission to use their extended UNIQUAC model.

## Notation

$aq$	Aqueous
$g$	Gas
$H$	Enthalpy, kJ
$h$	Specific enthalpy, kJ kg <sup>−1</sup>
$L$	Liquid
$l$	Liquid
$m$	Molality (mole per kg solvent)
$mol\%$	Mole percent
$P$	Pressure, bar
$Pr$	Pressure ratio
$q$	Vapor quality
$Q$	Heat transfer rate, MW
$s$	Specific entropy, kJ kg <sup>−1</sup> K <sup>−1</sup> /solid
$T$	Temperature, K
$V$	Vapor
$W$	Power, W

## Greek

$\alpha$	Nonrandomness factor
$\Delta$	Difference
$\eta$	Efficiency
$\tau$	Asymmetric binary interaction energy parameter

### Subscripts

calc	Calculated
cw	Waste stream
driving	Driving
exp	Experimental
<i>i,j</i>	Component
is	Isentropic
s	Constant entropy

### Abbreviations

COP	Coefficient of Performance
CRHP	Compression-resorption heat pump
e-NRTL	Electrolyte Non Random Two Liquid
EOS	Equation of State
HP	Heat pump
PC-SAFT	Perturbed Chain Statistical Association Fluid Theory
RK	Redlich-Kwong
SLE	Solid-liquid equilibrium
SRK	Soave-Redlich-Kwong
UNIQUAC	Universal Quasi Chemical
VCHP	Vapor compression heat pump
VLE	Vapor-liquid equilibrium

### References

- [1] Aspen Physical Property System. Aspen plus: rate-based model of the CO<sub>2</sub> capture process by NH<sub>3</sub> using aspen plus. Cambridge, MA: Aspen Tech; 2011.
- [2] Aspen Physical Property System. Aspen plus: rate-based model of the CO<sub>2</sub> capture process by NH<sub>3</sub> using aspen plus. Cambridge, MA: Aspen Tech; 2012.
- [3] Aspen Physical Property System. Version 8.8. Cambridge, MA: Aspen Tech; 2015.
- [4] Carlson EC. Don't gamble with physical properties for simulations. *Chem Eng Prog* 1996;92(10):35–46.
- [5] Chen CC, Britt HI, Boston JF, Evans LB. Local composition model for excess Gibbs energy of electrolyte systems. 1. Single solvent, single completely dissociated electrolyte systems. *AIChE J* 1982;28:588–96.
- [6] Choi YS, Nesić. Determining the corrosive potential of CO<sub>2</sub> transport pipeline in high pCO<sub>2</sub>-water environments. *Int J Greenh Gas Control* 2011;5:788–97.
- [7] Darde V. CO<sub>2</sub> capture using aqueous ammonia. PhD thesis. Technical University of Denmark; 2011.
- [8] Darde V, Thomsen K, van Well WJM, Bonalumi D, Valenti G, Macchi E. Comparison of two electrolyte models for the carbon capture with aqueous ammonia. *Int J Greenh Gas Control* 2012;8:61–72.
- [9] Darde V, Well WJ, Stenby EH, Thomsen K. Modeling of carbon dioxide absorption by aqueous ammonia solutions using the extended UNIQUAC model. *Ind. Eng Chem Res* 2010;49:12663–74.
- [10] European Council. 2030 Climate and energy policy framework. 2014.
- [11] European Environment Agency. Final energy consumption by sector and fuel. 2015. <http://www.eea.europa.eu/data-and-maps/indicators/final-energy-consumption-by-sector-9/assessment>. assessed November 2016.
- [12] Göppert U, Maurer G. Vapor-liquid equilibria in aqueous solutions of ammonia and carbon dioxide at temperatures up to 7 MPa. *Fluid Phase Equilibria* 1988;41:153–85.
- [13] IEA. Application of industrial heat pumps. Technical report. 2014.
- [14] Infante Ferreira CA, Zamfirescu C, Zaytsev D. Twin screw oil-free wet compressor for compression–absorption cycle. *Int J Refrig* 2006;29:556–65.
- [15] Itard LCM. Wet compression versus dry compression in heat pumps working with pure refrigerants or non-azeotropic mixtures. *Int. J Refrig* 1995;18:495–504.
- [16] Janecke E. Über die Löslichkeit von ammonbicarbonat in wasser bis zum schmelzpunkt. *Z für Electrochem* 1929;35:332–4.
- [17] Jensen JK, Markussen WB, Reinholdt L, Elmegaard B. On the development of high temperature ammonia-water hybrid absorption-compression heat pumps. *Int J Refrig* 2015a;58:79–89.
- [18] Jensen JK, Ommen T, Markussen WB, Reinholdt L, Elmgard B. Technical and economic working domains of industrial heat pumps: Part 2 – ammonia-water hybrid absorption-compression heat pumps. *Int J Refrig* 2015b;55:183–200.
- [19] Jilivero H, Jens KJ, Normann F, Andersson K, Halstensen M, Eimer D, et al. Equilibrium measurements of the NH<sub>3</sub>-CO<sub>2</sub>-H<sub>2</sub>O system-measurement and evaluation of vapor-liquid equilibrium data at low temperatures. *Fluid Phase Equilibria* 2015;385:237–47.
- [20] Kim YJ, You JK, Hong WH, Yi KB, Ko CH, Kim J. Characteristics of CO<sub>2</sub> absorption into aqueous ammonia. *Sep Sci Technol* 2008;43(4):766–77.
- [21] Kiss AA, Flores Landaeta SJ, Infante Ferreira CA. Towards energy efficient distillation technologies - making the right choice. *Energy* 2012;47:531–42.
- [22] Kiss AA, Infante-Ferreira CA. Heat pumps in chemical process industry. CRC-Press (Taylor & Francis Group), US; 2016.
- [23] Krzemien A, Więckol-Ryk A, Smoliński A. Assessing the risk of corrosion in amine-based CO<sub>2</sub> capture process. *J Loss Prev Process Ind.* 2016;43:189–97.
- [24] Kurz F, Rumpf B, Maurer G. Vapor-liquid-solid equilibria in the system NH<sub>3</sub>-CO<sub>2</sub>-H<sub>2</sub>O from around 310 to 470 K: New experimental data and modeling. *Fluid Phase Equilibria* 1995;104:261–75.
- [25] Lemmon EW, Huber ML, McLinden MO. NIST standard reference database 23: reference fluid thermodynamic and transport properties-REFPROP, version 9.1. Gaithersburg: National Institute of Standards and Technology, Standard Reference Data Program; 2013.
- [26] Lichtfers U. Spektroskopische Untersuchungen zur Ermittlung von Speziesverteilungen im System Ammoniak - Kohlendioxid - Wasser. PhD thesis. Kaiserslautern University of Technology; 2000.
- [27] Liu J, Gao HC, Peng CC, Wong DSH, Jang SS, Shen JF. Aspen Plus rate-based modeling for reconciling laboratory scale and pilot scale CO<sub>2</sub> absorption using aqueous ammonia. *Int J Greenh Gas Control* 2015;34:117–28.
- [28] Luo H, Bildea CS, Kiss AA. Novel heat-pump-assisted extractive distillation for bioethanol purification. *Ind. Eng Chem Res* 2015;54:2208–13.
- [29] Maribo-Mogensen B. Development of an electrolyte CPA equation of state for applications in the petroleum and chemical industries. PhD thesis. Technical University of Denmark; 2014.
- [30] Moran MJ, Shapiro HN. Fundamentals of engineering thermodynamics. sixth ed. John Wiley and Sons; 2010.
- [31] Müller G, Bender E, Maurer G. Das Dampf-Flüssigkeitsgleichgewicht des ternären Systems Ammoniak-Kohlendioxid-Wasser bei hohen Wassergehalten im Bereich zwischen 373 und 474 Kelvin. *Berichte Bunsenges für Phys Chem* 1988;92:148–60.
- [32] Niu Z, Guo Y, Zeng Q, Lin W. A novel process for capturing carbon dioxide using aqueous ammonia. *Fuel Process Technol* 2013;108:154–62.
- [33] Park H, Jung YM, You JK, Hong WH, Kim JN. Analysis of the CO<sub>2</sub> and NH<sub>3</sub> reaction in an aqueous solution by 2D IR COS: formation of bicarbonate and carbamate. *J Phys Chem A* 2008;112(29):6558–62.
- [34] Pawlikowski EM, Newman J, Prausnitz JM. Phase equilibria for aqueous solutions of ammonia and carbon dioxide. *Ind. Eng Chem Process Des Dev* 1982;21(4):764–70.
- [35] Pexton S, Badger EHM. E. H. M. The Examination of Aqueous solutions containing only NH<sub>3</sub> and CO<sub>2</sub>. *J Soc Chem Ind.* 1938;57:107–10.
- [36] Que H, Chen CC. Thermodynamic modeling of the NH<sub>3</sub>-CO<sub>2</sub>-H<sub>2</sub>O system with electrolyte NRTL model. *Ind. Eng Chem Res* 2011;50(19):11406–21.
- [37] Rumpf B, Weyrich F, Maurer G. Enthalpy changes upon partial evaporation of aqueous solutions containing ammonia and carbon dioxide. *Ind. Eng Chem Res* 1998;37:2983–95.
- [38] Shahandeh H, Jafari M, Kasiri N, Ivakpour J. Economic optimization of heat pump-assisted distillation columns in methanol-water separation. *Energy* 2015;80:496–508.
- [39] Shen HM. VLE measurement and calculation of NH<sub>3</sub>-H<sub>2</sub>O-CO<sub>2</sub>-N<sub>2</sub>-H<sub>2</sub> system under high pressure. *Huagong Xuebao* 1990;4:196–206.
- [40] N, Ten Asbroek, and G, Rexwinkel. (2016). Improved heat pump and process of heat pumping, Frames Renewable Energy Solutions BV., Patent application number N2016303.
- [41] Thomsen K, Rasmussen P. Modeling of vapor-liquid-solid equilibrium in gas-aqueous electrolyte systems. *Chem Eng Sci* 1999;54:1787–802.
- [42] Toporescu E. Sur la Préparation du bicarbonate de sodium. *Comptes Rendus* 1922;175:268–70.
- [43] Trypcu M, Kielkowska U. Solubility in the NH<sub>4</sub>HCO<sub>3</sub> + NaHCO<sub>3</sub> + H<sub>2</sub>O system. *J Chem Eng Data* 1998;43:201–4.
- [44] van de Bor DM, Infante Ferreira CA. Quick selection of industrial heat pump types including the impact of thermodynamic losses. *Energy* 2013;53:312–22.
- [45] van de Bor DM, Infante Ferreira CA, Kiss AA. Optimal performance of compression-resorption heat pump systems. *Appl Therm Eng* 2014;65:219–25.
- [46] van de Bor DM, Infante Ferreira CA, Kiss AA. Low grade waste heat recovery using heat pumps and power cycles. *Energy* 2015;89:864–73.
- [47] Van Duc Lon N, Lee M. A hybrid technology combining heat pump and thermally coupled distillation sequence for retrofit and debottlenecking. *Energy* 2015;81:103–10.
- [48] Vorster PPJ, Meyer JP. Wet compression versus dry compression in heat pumps working with pure refrigerants or non-azeotropic binary mixtures for different heating applications. *Int J Refrig* 2000;23:292–311.
- [49] Yanagisawa Y, Harano T, Imoto T. Vapor-liquid equilibrium for ternary system of ammonia-carbon dioxide-water at 70–99 °C. *Nippon Kagaku Kaishi* 1975;2:271–4.
- [50] Zhang M, Guo Y. A comprehensive model for regeneration process of CO<sub>2</sub> capture using aqueous ammonia solution. *Int J Greenh Gas Control* 2014;29:22–34.